Phototactic Clustering of Swimming Microorganisms in a Turbulent Velocity Field

Colin Torney and Zoltán Neufeld

School of Mathematical Sciences and Complex & Adaptive Systems Laboratory, University College Dublin, Belfield, Dublin 4, Ireland

(Received 12 February 2008; published 15 August 2008)

We study the distribution of swimming microorganisms advected by a two-dimensional smooth turbulent flow and attracted towards a light source through phototaxis. It is shown that particles aggregate along a dynamical attractor with fractal measure whose dimension depends on the strength of the phototaxis. Using an effective diffusion approximation for the flow, we derive an analytic expression for the increase in light exposure over the aggregate and by extension an accurate prediction for the fractal dimension based on the properties of the advection and the statistics of the attracting field.

DOI: 10.1103/PhysRevLett.101.078105 PACS numbers: 47.63.Gd, 05.45.−a, 47.27.−i, 87.18.Ed

The inhomogeneous distribution of chaotically advected particles has received much attention in a variety of contexts. It has been shown in the case of passive particles in compressible surface flow [1,2] and inertial particles in incompressible flow [3,4] that clusters form along a dynamical attractor of fractal measure. This intermittent distribution has important consequences for processes such as rain formation [5] and chemical or biological reaction processes [6,7]. In a biological context, microscale patchiness in plankton populations has been observed in several studies [8–11] and plays an important role in population dynamics and oceanic ecology.

In this Letter, we consider swimming particles advected by an incompressible flow with an effective compressibility induced by particle motility in the presence of an attracting light source. Particles detect the gradient of the illumination field and move in the direction of increasing light intensity with a swimming velocity proportional to the detected gradient. Motion is therefore governed by

$$\dot{\mathbf{r}} = \mathbf{v}_f(\mathbf{r}, t) + \chi \boldsymbol{\nabla} \Phi(\mathbf{r}), \tag{1}$$

where χ is the phototactic coefficient which defines the strength of a particle's reaction to the gradient of the illumination field $\Phi(\mathbf{r})$. For our simulations we assume a Gaussian light distribution, although results are not dependent on the exact functional form of $\Phi(\mathbf{r})$.

As a carrier flow, we use a synthetic model [12,13] which generates a Gaussian, isotropic, and homogeneous turbulent flow with a prescribed energy spectrum

$$E(k) \propto k^3 \exp\left[-\frac{3k^2}{2k_0^2}\right] \tag{2}$$

originally proposed by Kraichnan [14]. The flow is generated by using an Ornstein-Uhlenbeck process defined as the solution to the stochastic partial differential equation

$$\frac{\partial \psi}{\partial t} = \nu \nabla^2 \psi + \sqrt{\xi} \frac{\partial W}{\partial t}, \tag{3}$$

where ψ is the stream function of the velocity field, ν is a parameter which sets the decay time of spatial structure, ξ represents the magnitude of the stochastic forcing, and W is a Wiener process. Following [13], we introduce the length scale L and time scale T such that $T = L\sqrt{\nu/\xi}$ and rescale so that the flow is periodic on a square domain with unit length. The length scale of the highest energy modes is defined by $2\pi/k_0$ and we set this to be two thirds of the box size. The spectrum is normalized which leads to a mean squared velocity of the flow of 0.5. For the illumination field, we use a Gaussian function defined as $\Phi(\mathbf{r}) = \exp[-8(x^2 + y^2)/L^2]$.

In an ergodic incompressible flow with no transport barriers an ensemble of passively advected particles are quickly dispersed into a spatially uniform density distribution. Conversely, phototactic particles swimming in the direction of a fixed illumination gradient in the absence of advection would concentrate in regions of maximum light intensity. When combined, these two effects result in a highly nonuniform, statistically stationary steady state. Distributions in this regime are shown in Fig. 1 while animations are included as supplementary material [15]. Particles do not converge to a point, as would be the case for strong phototactic attraction, but instead aggregate along a dynamical fractal attractor and continue to visit all regions of the physical space.

Despite this, the average illumination received by the ensemble of particles (or equivalently along the trajectory of a single particle) increases with χ and is higher than the spatial average illumination. In Fig. 2 we show the time-averaged increase in light exposure of an ensemble of phototactic particles as compared to passively advected nonmotile particles as a function of the phototactic coefficient. This value saturates as particles spend longer in the region of maximum light intensity until for large values of χ all particles collect in a single point.

As χ is increased, the attractor becomes more singular with most particles concentrated in thin filaments separated by empty regions. To quantify the characteristics of the attractor we numerically calculate the information dimension [16] which quantifies the degree to which the fractal fills the domain and indicates self-similar structure over a

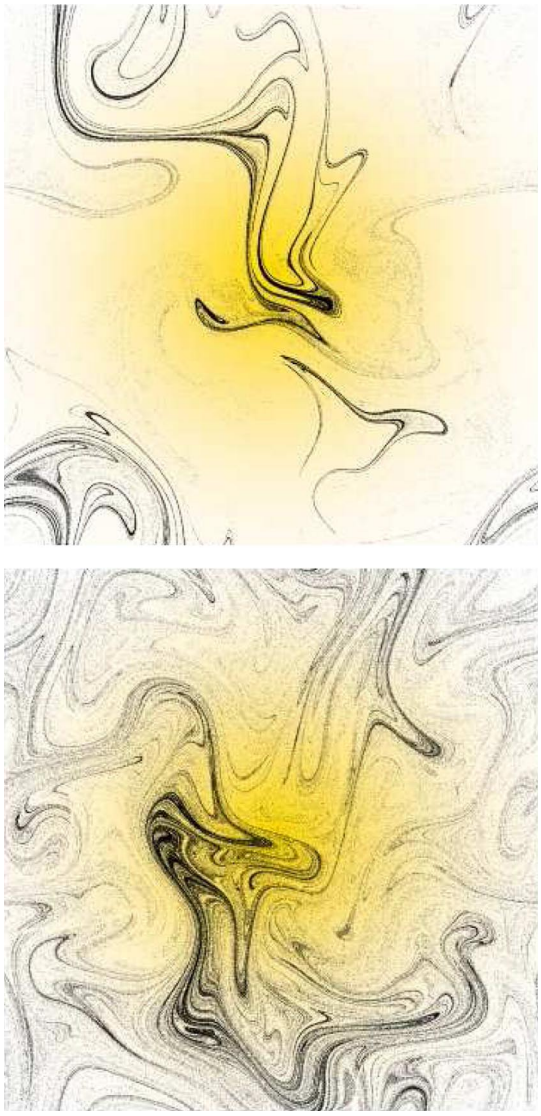

FIG. 1 (color online). Distribution of 500 000 phototactic particles after relaxation of transients. Top: $\chi = 0.15$. Bottom: $\chi = 0.05$. Light distribution is shown in yellow (shaded light gray region).

broad range of scales. Results for various values of χ are shown in Fig. 2.

In order to investigate the relationship between χ and both the average illumination gain of the aggregate and the fractal dimension of the attractor, we approximate the turbulent advection as a purely diffusive process.

Although the instantaneous dynamical attractor changes in an irregular fashion following the turbulent flow, by averaging over time we can obtain a picture of the denser regions of the physical space which will then allow us to quantify various statistical properties of the system. To this end, we define $\bar{\rho}$ as the time-averaged density of particles at a given point in space and the notation $\langle \cdots \rangle_{\bar{\rho}}$ to mean an average quantity defined over $\bar{\rho}$. With these definitions and an effective diffusion approximation for the flow, we model

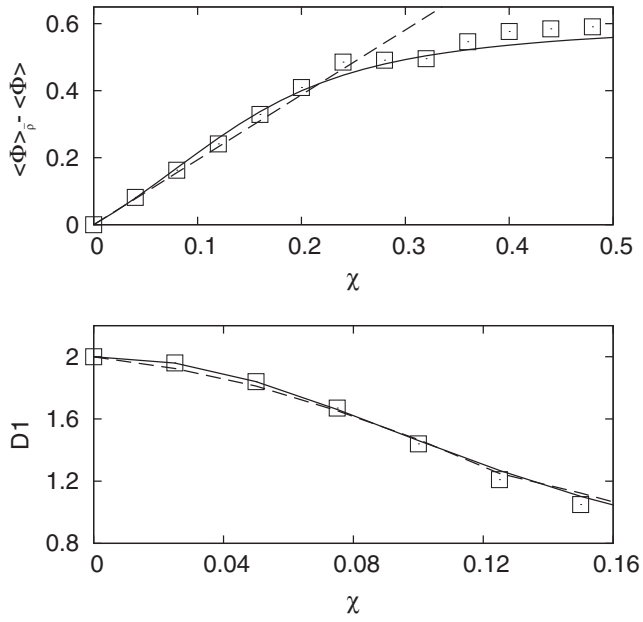

FIG. 2. Top: Gain in light exposure. Squares—numerical results, solid line—theoretical approximation, dashed line—first order theoretical approximation. Bottom: Information dimension. Squares—values calculated from distribution by weighted box count [16], dashed line—results from numerically calculated Lyapunov exponents, solid line—theoretical model.

the system by the equation

$$\frac{\partial \bar{\rho}}{\partial t} = D_f \nabla^2 \bar{\rho} - \boldsymbol{\nabla} \cdot (\bar{\rho} \chi \boldsymbol{\nabla} \Phi), \tag{4}$$

where D_f is the effective diffusivity of the flow defined by the asymptotic dispersion rate of advected passive particles in an unbounded domain as $\langle d^2 \rangle \simeq 4 D_f t$. We calculate this quantity numerically and use the value obtained in the subsequent results. The first term on the right-hand side of Eq. (4) represents the diffusive effect of the turbulent flow which smooths out any inhomogeneities in the distribution and if dominant would lead to a uniform particle density. The second term counteracts this effect by collecting particles in high light intensity regions leading to a nonuniform distribution. Equation (4) has a steady state solution of the form

$$\bar{\rho}(\mathbf{r}) = \frac{1}{Z} \exp\left[\frac{\chi}{D_f} \Phi(\mathbf{r}) \right], \tag{5}$$

which is analogous to a Boltzmann distribution of noninteracting particles in an external field, where Z is a normalization factor akin to a partition function which allows us to use $\bar{\rho}$ as a probability density. Equation (5) is a valid approximation when the flow can be modeled as diffusion. This precludes illumination gradients which result in swimming speeds that dominate the flow velocity and which vary on a length scale smaller than the flow correlation length as at these scales advection dominates.

To compare this result with numerical experiments we note that as a result of radial symmetry in the illumination field the particle distribution is also radially symmetric. This is not consistent with the boundary conditions but is an accurate approximation when neglecting the corner regions. The two dimensional distribution can then be fully described by a one dimensional radial profile. In Fig. 3, the result predicted from Eq. (5) is compared to a time-averaged normalized histogram plot of the radial location of particles for $\chi = 0.05$. We also include in Fig. 3 a scatter plot of results against expected values for a range of χ which illustrates the excellent agreement of numerics with the effective diffusion approximation.

Using the distribution given above we can evaluate the average light intensity experienced by particles with a given phototactic response parameter χ as

$$\langle \Phi \rangle_{\bar{\rho}} = \frac{1}{Z} \int^{V} \exp\left[\frac{\chi}{D_f} \Phi(\mathbf{r}) \right] \Phi(\mathbf{r}) dV, \tag{6}$$

which can be rewritten as

$$\langle \Phi \rangle_{\bar{\rho}} = D_f \frac{\partial \log Z}{\partial \chi}. \tag{7}$$

As Z is an expectation value over the unit area domain the logarithmic term can be treated as a cumulant generating function of the light distribution Φ. This gives

$$\langle \Phi \rangle_{\bar{\rho}} = \sum_{n=0}^{\infty} \kappa_{n+1} \frac{1}{n!} \left(\frac{\chi}{D_f} \right)^n, \tag{8}$$

where κ_n are the cumulants of the illumination field. For weakly phototactic particles, i.e., $\chi / D_f \ll 1$, the higher order terms can be neglected leaving

$$\langle \Phi \rangle_{\bar{\rho}} \simeq \langle \Phi \rangle + \frac{\chi}{D_f} (\langle \Phi^2 \rangle - \langle \Phi \rangle^2). \tag{9}$$

This explains the linear relationship seen in Fig. 2 for small values of χ and shows that the gain in illumination exposure due to phototaxis is proportional to the variance of the illumination field. The truncated series is plotted in Fig. 2 alongside results containing higher order terms required for convergence.

Interestingly, the time-averaged distribution defined by Eq. (5) can also be used to calculate the dimension of the dynamical attractor. The Kaplan-Yorke conjecture [17] relates the information dimension of an attractor to the average stretching and contraction rates in the phase space by the formula (for two-dimensional phase space)

$$D_1 = 1 + \frac{\lambda_1}{|\lambda_2|}, \tag{10}$$

where λ_1, λ_2 are the Lyapunov exponents of the system. The sum of the Lyapunov exponents defines a dissipation rate α, i.e., the average rate at which volumes in the phase space contract. In a conservative system, as is the case of particles passively advected by an incompressible flow, α is zero and therefore in the two-dimensional model $\lambda_1 = -\lambda_2$ and the information dimension is two. However, if phototaxis is present particles no longer follow the streamlines of the flow and there is a net contraction in the system which reduces the dimension of the attractor.

The Lyapunov exponents can be determined numerically by a method proposed by Benettin [18] and the values found in this way show the dependence of λ_1, λ_2, and α on the phototactic coefficient (Fig. 4). The information dimension can now be found by using the Kaplan-Yorke

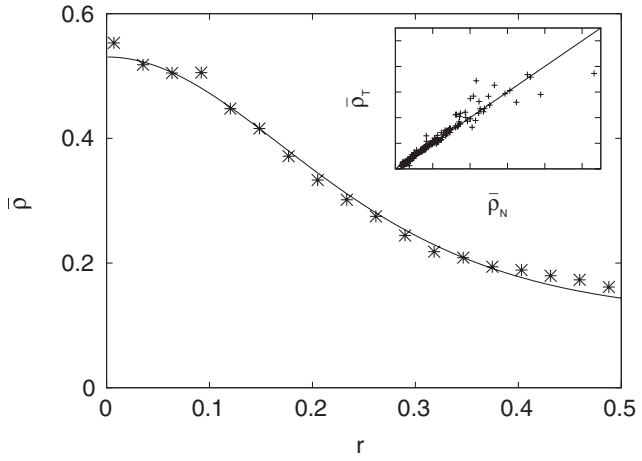

FIG. 3. Radial plot of probability density function (solid line) and numerical results (points) for average particle distribution, $\chi = 0.05$. Inset: Scatter plot of predicted density ($\bar{\rho}_T$) to numerically observed density ($\bar{\rho}_N$) for range of χ from 0.025 to 0.15. Points lying on the diagonal represent exact match between effective diffusion model and numerics.

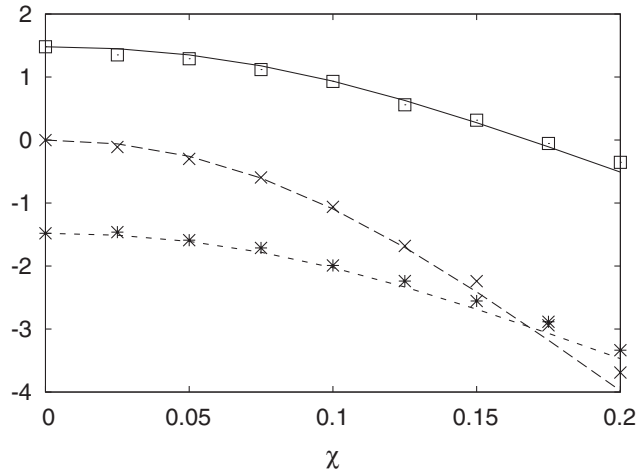

FIG. 4. Lyapunov exponents and dissipation rate. Symbols represent numerical values found by the Benettin method, line values calculated from the theoretical approximation defined by Eqs. (11) and (12). Squares and solid line represent λ_1; crosses and heavy dashed line represent α; asterisks and fine dashed line represent λ_2.

conjecture and this agrees with the values calculated directly from the particle distributions as shown in Fig. 2. We include values of dimension greater than 1 as at higher values of χ the Kaplan-Yorke conjecture does not hold. In this regime both Lyapunov exponents are negative and this results in a distribution which converges to a point or is intermittently stretched into a line.

Returning to the theoretical model, the rate α can be obtained from the divergence of the particles' velocity fields. Because of the incompressibility of the carrier flow

$$\alpha = \langle \chi \nabla^2 \Phi \rangle_{\bar{\rho}} = \int^V \bar{\rho} \chi \nabla^2 \Phi(\mathbf{r}) dV, \tag{11}$$

where by ergodicity averaging over a single trajectory over long times is taken to be equivalent to the weighted average over the distribution $\bar{\rho}$ previously defined in our continuum description.

From the isotropic properties of the flow and no correlation between fluid and illumination field, we expect the contraction of phase space elements due to phototaxis to have an equal effect on both Lyapunov exponents. This is consistent with numerical results as shown in Fig. 4. Defining λ_0 as the positive exponent of the carrier flow (i.e., in the case of passive particles $\lambda_1 = \lambda_0$, $\lambda_2 = -\lambda_0$) the exponents for the particles are then

$$\lambda_1 = \lambda_0 + \frac{1}{2}\langle \chi \nabla^2 \Phi \rangle_{\bar{\rho}} \qquad \lambda_2 = -\lambda_0 + \frac{1}{2}\langle \chi \nabla^2 \Phi \rangle_{\bar{\rho}}. \tag{12}$$

For the Gaussian light distribution, the integral in Eq. (11) can be evaluated numerically and values for λ_1, λ_2, and α are plotted in Fig. 4 alongside those obtained from the Benettin method. Combining Eqs. (10)–(12) gives an expression for the fractal dimension of the distribution in terms of Φ, χ, and the properties of the carrier flow field λ_0 and D_f.

$$D_1 = \left(\frac{1}{2} - \frac{1}{4\lambda_0 Z} \int^V \exp\left[\frac{\chi}{D_f} \Phi \right] \chi \nabla^2 \Phi dV \right)^{-1}. \tag{13}$$

To illustrate their agreement with the numerical results, solutions to this equation are included in Fig. 2.

An alternative formulation can be obtained from Eq. (11) by the use of integration by parts

$$\alpha = \oint^S \bar{\rho} \chi \boldsymbol{\nabla} \Phi dS - \int^V \frac{\bar{\rho}}{D_f} (\chi \boldsymbol{\nabla} \Phi)^2 dV, \tag{14}$$

where the boundary term vanishes for most boundary conditions (i.e., smooth periodic or no-flux illumination field) [19]. The second integral demonstrates that α is always negative and is proportional to the mean square swimming velocity of the phototactic particles. Thus the information dimension can be written as

$$D_1 = 2\left[1 + \frac{\langle V_s^2 \rangle}{2\lambda_0 D_f} \right]^{-1}. \tag{15}$$

In a fully chaotic flow, the effective diffusivity can be estimated as $D_f \sim UL$ and the Lyapunov exponent is an inverse characteristic time scale of the flow $\lambda_0 \sim U/L$. Using these relations, Eq. (15) shows that the information dimension is a function of the nondimensional ratio of the average kinetic energy of swimming measured relative to that of the carrier flow.

The combined effect of phototaxis and turbulent flow leads to highly nonuniform distribution of microorganisms and this provides a plausible mechanism for the generation of microscale patchiness observed in experiments [8–11]. The relationship of the dimensionality of the distribution to the measurable kinetic energy of the swimming organisms may in the future be used by evaluating the statistical properties of the microorganism swimming energy and the degree of aggregation due to taxis to predict or confirm measurable spatial structure.

This work was supported by Science Foundation Ireland. Computational facilities provided by ICHEC.

[1] J. C. Sommerer and E. Ott, Science **259**, 335 (1993).
[2] G. Boffetta, J. Davoudi, B. Eckhardt, and J. Schumacher, Phys. Rev. Lett. **93**, 134501 (2004).
[3] J. Bec, J. Fluid Mech. **528**, 255 (2005).
[4] K. Duncan, B. Mehlig, S. Östlund, and M. Wilkinson, Phys. Rev. Lett. **95**, 240602 (2005).
[5] G. Falkovich, A. Fouxon, and M. G. Stepanov, Nature (London) **419**, 151 (2002).
[6] Z. Toroczkai, G. Károlyi, A. Péntek, T. Tél, and C. Grebogi, Phys. Rev. Lett. **80**, 500 (1998).
[7] G. Károlyi, Á. Péntek, I. Scheuring, T. Tél, and Z. Toroczkai, Proc. Natl. Acad. Sci. U.S.A. **97**, 13 661 (2000).
[8] A. Tsuda, J. Oceanography **51**, 261 (1995).
[9] L. Seuront and Y. Lagadeuc, J. Plankton Res. **23**, 1137 (2001).
[10] J. R. Seymour, J. G. Mitchell, L. Pearson, and R. L. Waters, Aquat. Microb. Ecol. **22**, 143 (2000).
[11] R. L. Waters and J. G. Mitchell, Mar. Ecol. Prog. Ser. **237**, 51 (2002).
[12] A. C. Martí, J. M. Sancho, F. Sagués, and A. Careta, Phys. Fluids **9**, 1078 (1997).
[13] H. Sigurgeirsson and A. M. Stuart, Phys. Fluids **14**, 4352 (2002).
[14] R. H. Kraichnan, Phys. Fluids **13**, 22 (1970).
[15] See EPAPS Document No. E-PRLTAO-101-023830 for animations of further values of χ. For more information on EPAPS, see http://www.aip.org/pubservs/epaps.html.
[16] E. Ott, *Chaos in Dynamical Systems* (Cambridge University Press, Cambridge, England, 1993).
[17] J. L. Kaplan and J. A. Yorke, Lect. Notes Math. **730**, 228 (1979).
[18] G. Benettin, L. Galgani, and J.-M. Strelcyn, Phys. Rev. A **14**, 2338 (1976).
[19] Note: This condition is not exactly satisfied in our numerical simulations as the Gaussian illumination field has a small discontinuity in the gradient at the boundaries.